How S–C–N anomeric effects and energetic preference across [S–C–C–O] fragments steer conformational equilibria in 4′-thionucleosides. ^{1}H NMR and *ab initio* MO study †

Martin Črnugelj,[a] David Dukhan,[b] Jean-Louis Barascut,[b] Jean-Louis Imbach[b] and Janez Plavec *[a]

[a] *National Institute of Chemistry, Hajdrihova 19, SI-1115 Ljubljana, Slovenia*
[b] *Laboratoire de Chimie Bio-Organique, UMR-5625-CNRS, Université de Montpellier II, 34095 Montpellier Cedex 5, France*

Received (in Cambridge, UK) 8th October 1999, Accepted 3rd November 1999

Variable temperature- and pH-dependent ^{1}H NMR conformational analyses of $^3J_{HH}$ coupling constants and NOE enhancements in the 4′-thionucleosides **1**–**10** in D_2O, complemented by *ab initio* calculations, have given insight into the interplay of anomeric and other stereoelectronic effects that are modulated by the substitution of ring oxygen by sulfur in natural nucleosides. The N⇌S pseudorotational equilibrium of the 2′-deoxy-4′-thionucleosides **1**–**4** is slightly shifted towards S-type conformers, while their ribo analogues **5**–**8** exhibit *ca.* 50 : 50 ratio at 278 K and neutral pH. α-4′-Thionucleosides **9** and **10** display a strong preference for N-type conformers. The S–C–N anomeric effect in **1**–**4** is stronger in purine than in pyrimidine 4′-thionucleosides, which is opposite to natural 4′-oxonucleosides, and increases in the following order: thymine < cytosine < guanine < adenine. The S–C–N anomeric effect in **1**–**4** is weaker than the O–C–N anomeric effect in their 4′-oxo counterparts. We have observed considerable population of up to 40% of γ^- rotamers across the C4′–C5′ bond, which has been attributed to the preference of the [S4′–C4′–C5′–O5′] fragments in **1**–**10** for *trans* over *gauche* conformation. Similarly, the 3′-OH group drives the N⇌S equilibrium in **1**–**10** towards N where the [S4′–C4′–C3′–O3′] fragment adopts *trans* conformation. The 2′-OH group has been found to preferentially stabilise N-type sugar conformation in the 4′-thioribonucleosides **5**–**8** where it occupies a pseudoaxial orientation. The pK_a values in **1**–**10** are almost identical to the pK_a values of their natural counterparts, which shows that the acid–base character of the constituent heterocyclic moieties does not change upon substitution of oxygen with sulfur atom. The shift of the N⇌S pseudorotational equilibrium in **1**–**8** towards N upon protonation and towards S upon deprotonation of the nucleobase is smaller by up to 10 percentage points in comparison to their 4′-oxo counterparts. This can be attributed to less efficient tuning of the S–C–N anomeric effect in **1**–**8** by protonation and deprotonation of the nucleobase. 1D difference NOE experiments indicated predominant *anti* orientation of the nucleobase in **2**–**10**. *Ab initio* calculations at up to MP2/6-31G**//6-31G** level have shown two energy minima in the North and South regions of conformational space with the energy barriers between 17.5 and 28.5 kJ mol^{-1} in the East region. Interestingly, the energy barrier in the West region is comparable or even lower than the barrier in the East region of conformational space in **1**–**10**, which is in contrast to natural nucleosides.

Introduction

The substitution of the ring oxygen atom with sulfur in nucleoside analogues has been extensively investigated as means to derive potential antiviral and antitumour drugs.[1–3] In addition to the structural changes caused by C–S bonds being longer than C–O bonds, the introduction of a sulfur atom has many other implications, like resistance to *N*-glycosidic bond hydrolysis by nucleoside phosphorylases,[4] and perturbation in the electronic environment of the heterocyclic ring due to the lower electronegativity of sulfur relative to oxygen. 4′-Thio-β-D-oligoribonucleotides are a promising class of antisense agents which exhibit improved stability toward nuclease degradation while retaining specific hybridisation with complementary RNA target sequences and favourable thermal stability.[5–10] The endocyclic oxygen-to-sulfur substitution also influences the ability of modified oligonucleotides to serve as substrates for enzymes by changing groove dimensions of the hybrid duplex.

The D-ribo or D-2′-deoxyribofuranose moieties in natural nucleosides are involved in a two-state conformational equilibrium between two distinctly identifiable North (N) and South (S) conformations which interconvert fast on the NMR time scale.[11–13] The two-state N⇌S pseudorotational equilibrium in solution is controlled by the competing anomeric and *gauche* effects.[14] The 2′-OH and 3′-OH groups drive the N⇌S equilibrium by a tendency to adopt a *gauche* arrangement of O–C–C–O fragments with O4′–C1′/C4′ bonds.[15] The heterocyclic bases in *N*-nucleosides drive the two-state N⇌S pseudorotational equilibrium of the constituent β-D-pentofuranosyl moieties by two counteracting contributions from (i) the inherent steric effect of the nucleobase[16] and (ii) the anomeric effect.[17–19]

We have initiated a conformational study of a series of β-D-2′-deoxy-4′-thioribonucleosides **1**–**4**, their ribo counterparts **5**–**8** and α-D-4′-thioribonucleosides **9** and **10** in order to assess how the electronic changes caused by replacement of oxygen with sulfur change the stereoelectronic effects which govern their conformational degrees of freedom and possibly perturb the pK_a values. The conformational preferences of **1**–**10** in aqueous solutions were examined with the use of temperature- and pH-dependent ^{1}H NMR spectroscopy. Our previous study has shown that 4′-thiothymidine (**4**) and its 5-bromovinyl

† Supplementary data is available for this paper. For direct electronic access see http://www.rsc.org/suppdata/p2/2000/a908096a, otherwise available from BLDSC (SUPPL. NO. 57683, pp.) or the RSC Library. See Instructions for Authors available *via* the RSC web page (http://www.rsc.org/authors).

Table 1 The N⇌S pseudorotational equilibrium in **1**–**10**[a]

Compound	Protonation site	pH	P_N	Ψ_m^N	P_S	Ψ_m^S	Rms	ΔJ_{max}	%S 278 K	%S 358 K
β-tdA (**1**)	Prot.	1.8	5.4	47.0[b]	170.3	47.0[b]	0.07	0.1	57	57
	Neutral	6.8	−0.5	46.0[b]	185.2	46.0[b]	0.09	0.2	56	58
β-tdG (**2**)	Prot.	0.7	2.2	41.0[b]	171.1	41.0[b]	0.12	0.2	43	46
	Neutral	6.7	10.9	39.0[b]	150.6	39.0[b]	0.18	0.3	62	61
	Deprot.	11.8	8.9	38.0[b]	149.1	38.0[b]	0.12	0.3	60	60
β-tdC (**3**)	Prot.	2.0	9.1	42.0[b]	170.8	42.0[b]	0.07	0.2	64	61
	Neutral	6.5	15.5	43.0[b]	169.7	43.0[b]	0.05	0.1	64	61
β-tdT (**4**)	Neutral	6.7	19.6	43.0[b]	169.5	43.0[b]	0.06	0.1	71	66
	Deprot.	11.9	21.4	43.0[b]	168.5	43.0[b]	0.05	0.1	71	66
β-tA (**5**)	Prot.	1.5	0.7	45.0[b]	151.6	45.0[b]	0.03	0.1	51	58
	Neutral	7.8	10.0	44.0[b]	158.3	44.0[b]	0.05	0.1	52	59
β-tG (**6**)	Prot.	0.7	24.9	45.0[b]	176.2	45.0[b]	0.07	0.1	34	50
	Neutral	7.6	−0.1	45.0[b]	151.0	45.0[b]	0.05	0.1	54	58
	Deprot.	11.2	11.0	44.0[b]	157.0	44.0[b]	0.05	0.1	59	60
β-tC (**7**)	Prot.	1.4	14.1	44.0[b]	155.9	44.0[b]	0.06	0.1	46	55
	Neutral	6.9	6.1	45.0[b]	147.5	45.0[b]	0.06	0.2	46	52
β-tU (**8**)	Neutral	7.4	13.1	44.0[b]	155.6	44.0[b]	0.04	0.1	55	60
	Deprot.	11.7	15.1	44.0[b]	154.0	44.0[b]	0.04	0.1	53	56
α-tA (**9**)	Prot.	1.7	−1.1	43.0[b]	188.6	44.0[b]	0.05	0.1	37	43
	Neutral	7.2	3.6	44.5	180.0[b]	44.0[b]	0.07	0.1	19	29
α-tU (**10**)	Neutral	7.5	7.2	44.1	180.0[b]	44.0[b]	0.05	0.1	16	24
	Deprot.	11.6	6.4	45.8	180.0[b]	44.0[b]	0.07	0.2	0	11

[a] The puckering parameters P_N, P_S, Ψ_m^N and Ψ_m^S are given in degrees, rms error and ΔJ_{max} are in Hz. [b] The pseudorotational parameter was kept fixed during iterative optimisation procedure.

analogue adopt nearly equivalent N⇌S equilibria, as does natural nucleoside.[20] A quantitative evaluation of $\Delta H°$ of pyrimidine *vs.* purine aglycon through a comparison of the respective $\Delta H°$ values of the N⇌S pseudorotational equilibria of **1**–**10** has given us a broader insight into the energetic strength of the S4′–C1′–N9 *vs.* O4′-C1′–N9 anomeric effects in 2′-deoxyribonucleosides. The replacement of O4′ with sulfur is, in addition, influencing the population of γ-rotamers and the driving of the N⇌S equilibrium by the 3′-OH group through the energetic preference along [S–C–C–O] fragments in **1**–**10**.

Results and discussion

^{1}H NMR analysis of dynamic conformational equilibria of 4′-thionucleosides 1–10 in solution

The solution conformation of **1**–**10** has been inferred from $^3J_{HH}$ coupling constants and 1D difference NOE enhancements which have been acquired as a function of temperature from 278 to 358 K in 20 K steps and as a function of pH from 0.3 to 12.3 in steps of *ca*. 0.5 units (Table S1). $^3J_{4'5'}$ and $^3J_{4'5''}$ coupling constants were interpreted with the use of the generalised Karplus–Altona equation, which accounted for the substitution of O4′ in the natural pentofuranosyl moiety with a sulfur atom in **1**–**10**. (Table S2).[21,22] The analysis of the solution conformation of the sugar moieties in **1**–**10** was based on $^3J_{1'2'}$, $^3J_{1'2''}$, $^3J_{2'3'}$, $^3J_{2'3''}$ and $^3J_{3'4'}$ proton–proton coupling constants, which were interpreted in terms of a two-state N⇌S pseudorotational equilibrium with the use of the computer program PSEUROT.[23] Particular care has been taken in the interpretation of $^3J_{HH}$ coupling constants to account for the presence of sulfur as one of the substituents along H–C–C–H coupling networks in **1**–**10**.[21,22] Parameters *A* and *B*, which relate[24] proton–proton torsion angles and the corresponding endocyclic torsion angles, have been determined for **1**–**10** with the use of *ab initio* optimised geometries at the HF/3-21G level (Table S3). The parameters a_j and ε_j in eqn. (1) are the required

$$v_j = a_j \times \Psi_m \times \cos[P + \varepsilon_j + 4\pi/5 \times (j - 2)] \quad 0 \le j \le 4 \quad (1)$$

corrections[25] due to the unequilateral 4′-thiopentofuranosyl ring and have been calculated from a large set of *ab initio* optimised geometries (Table S4).

$^3J_{HH}$ Coupling constants in **1**–**4** have been interpreted by constraining Ψ_m^N and Ψ_m^S to fixed values between 39 and 46° while optimising the phase angles of pseudorotation and populations of N- and S-type pseudorotamers. After convergence we obtained the best fits between experimental and back-calculated $^3J_{HH}$ (root-mean-square error < 0.18 Hz, ΔJ_{max} < 0.3 Hz) for the N⇌S pseudorotational equilibria in **1**–**4** (Table 1). Conformational analysis of β-tdA (**1**) has been hampered because of isochronicity of H2′ and H2″ resonances even at 600 MHz and the sum of coupling constants for H1′ and H3′ has been used. Similarly, conformational analyses of $^3J_{HH}$ coupling constants in **5**–**8** have been performed by constraining Ψ_m^N and Ψ_m^S to fixed values of 44 and 45°, which have given the best fits (root-mean-square error < 0.06 Hz, ΔJ_{max} < 0.2 Hz) for the N⇌S conformational equilibria in **5**–**8** (Table 1). A high preference for N-type pseudorotamers of 81 and 84% has been found for α-tA (**9**) and α-tU (**10**) at 278 K at neutral pH by constraining P_S and Ψ_m^S (Table 1).

The populations of individual conformers at five temperatures in the range from 278 to 358 K in 20 K steps have been used to calculate the enthalpy and entropy of the N⇌S pseudorotational equilibrium in **1**–**10** by making van't Hoff plots. The Pearson correlation coefficients between $\ln(x_S/x_N)$ and reciprocal of temperature were higher than 0.960. β-tdA (**1**)

Table 2 Thermodynamic parameters for the N⇌S pseudorotational equilibrium in 4′-thionucleoside analogues **1**–**10** in D_2O[a]

Compound	Protonation state	pH	$\Delta H°$	$\Delta S°$	$-T\Delta S°$	$\Delta G°$
β-tdA (**1**)	Prot.	1.8	0.0 (0.1)	2.2 (0.2)	−0.7	−0.7 (0.1)
	Neutral	6.8	0.8 (0.1)	4.9 (0.6)	−1.5	−0.7 (0.1)
β-tdG (**2**)	Prot.	0.7	1.1 (0.1)	1.7 (0.3)	−0.5	0.6 (0.1)
	Neutral	6.7	−0.7 (0.1)	1.7 (0.1)	−0.5	−1.2 (0.1)
	Deprot.	11.8	−0.4 (0.1)	2.1 (0.1)	−0.6	−1.0 (0.1)
β-tdC (**3**)	Prot.	2.0	−1.6 (0.1)	−0.9 (0.1)	0.3	−1.3 (0.1)
	Neutral	6.5	−1.4 (0.1)	−0.3 (0.1)	0.1	−1.3 (0.1)
β-tdT (**4**)	Neutral	6.7	−2.7 (0.1)	−2.2 (0.1)	0.7	−2.0 (0.1)
	Deprot.	11.9	−2.3 (0.1)	−1.0 (0.1)	0.3	−2.0 (0.1)
β-tA (**5**)	Prot.	1.5	2.9 (0.1)	10.8 (1.6)	−3.2	−0.3 (0.4)
	Neutral	7.8	2.9 (0.2)	11.1 (2.3)	−3.5	−0.6 (0.6)
β-tG (**6**)	Prot.	0.7	6.6 (0.3)	18.4 (2.1)	−5.5	1.1 (0.1)
	Neutral	7.6	1.5 (0.1)	6.8 (1.6)	−2.0	−0.5 (0.4)
	Deprot.	11.2	0.3 (0.1)	4.2 (1.2)	−1.2	−0.9 (0.4)
β-tC (**7**)	Prot.	1.4	4.0 (0.2)	13.0 (1.6)	−3.9	0.1 (0.5)
	Neutral	6.9	2.4 (0.1)	7.3 (0.1)	−2.2	0.2 (0.1)
β-tU (**8**)	Neutral	7.4	2.2 (0.1)	9.6 (1.5)	−2.9	−0.7 (0.4)
	Deprot.	11.7	1.3 (0.1)	5.8 (1.2)	−1.7	−0.4 (0.4)
α-tA (**9**)	Prot.	1.7	2.5 (0.3)	4.7 (0.4)	−1.4	1.1 (0.5)
	Neutral	7.2	6.1 (0.5)	9.7 (1.0)	−2.9	3.2 (0.2)
α-tU (**10**)	Neutral	7.5	5.5 (0.6)	5.7 (1.4)	−1.7	3.8 (0.2)

[a] The $\Delta H°$, $-T\Delta S°$ (at 298 K) and $\Delta G°$ are in kJ mol^{-1}, $\Delta S°$ are in J mol^{-1} K^{-1}. The standard deviations (σ) in $\Delta H°$, $\Delta S°$ and $\Delta G°$ are in parentheses.

exhibits a small positive $\Delta H°$ value, which is, at 298 K, opposed by an entropy contribution twice as strong (Table 2). 4′-Thio-2′-deoxyribonucleosides **2**–**4** are characterised by negative $\Delta H°$ values, which denote stabilisation of S-type sugar conformation (Table 2). $\Delta H°$ and the counteracting entropy contributions are of comparable strength in **5**–**8** at 298 K, which results in *ca.* 1 : 1 ratio of N and S conformers (Table 2). N-Type conformations of α-tA (**9**) and α-tU (**10**) are stabilised by $\Delta H°$ values of 6.1 and 5.5 kJ mol^{-1}, which are opposed by weaker entropy contributions (Table 2).

The energetic preference of [S–C–C–O] fragments drives $\gamma^+ \rightleftharpoons \gamma^t \rightleftharpoons \gamma^-$ and N⇌S conformational equilibria in 1–10

The conformational equilibrium across the C4′–C5′ bond and the N⇌S pseudorotational equilibria in **1**–**10** are driven by the following 1,4 interactions involving sulfur atom: [S4′–C4′–C5′–O5′] and [S4′–C4′–C3′–O3′] fragments in 2′-deoxy-4′-thionucleosides **1**–**4**, and additionally by [S4′–C1′–C2′–O2′] fragments in their ribo analogues **5**–**10**. It is well established that [O–C–C–O] fragments in 4′-oxonucleosides prefer *gauche* over *trans* conformations and are responsible, for example, for the preference for S-type sugar conformations in 2′-deoxynucleosides.[15] As the sulfur atom is less electronegative than oxygen a much weaker, if any, *gauche* effect is expected for [S–C–C–O] fragments. Our pilot *ab initio* calculations at MP2/6-311++G** level on 2-methylthioethanol showed a preference of 1.4 kJ mol^{-1} for *trans* over *gauche* conformation.[26] The linear calibration graphs of $\Delta H°$ of the *gauche* effects of [O4′–C4′–C3′–X3′] fragments in 3′-substituted-2′,3′-dideoxythymidines and the group electronegativities of the 3′-substituents according to Mullay's[27] and Inamoto's[28] scales suggest that [S–C–C–O] fragments prefer *trans* over *gauche* conformation by 0.9 and 1.1 kJ mol^{-1}, respectively.

Interpretation of the experimental $^3J_{4'5'}$ and $^3J_{4'5''}$ coupling constants has shown that the population of γ^- rotamers is between 23 and 40 percentage points in **1**–**8** at 278 K and neutral pH (Table S2). Pairwise comparisons have shown that the

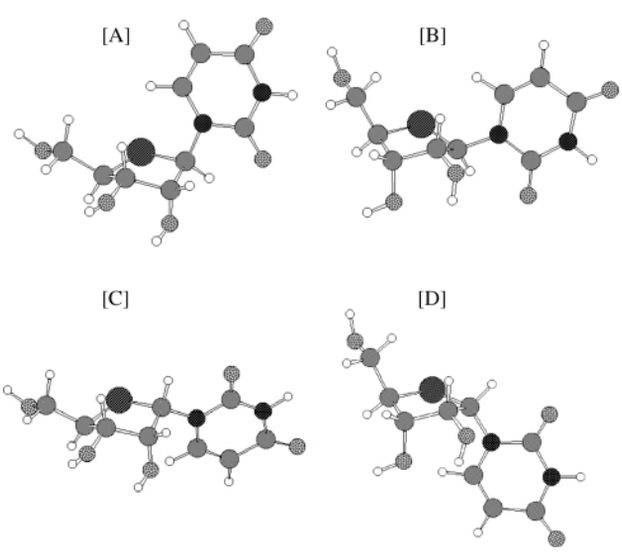

Fig. 1 Models of β-tU (**8**) in panels [A] and [B], and α-tU (**10**) in panels [C] and [D], obtained by completely free *ab initio* optimisations at HF/6-31G** level of theory, in the North (panels [A] and [C]) and South (panels [B] and [D]) regions of conformational space showing the relative positions of the exocyclic substituents of 4′-thiopentofuranosyl moiety. Structural details of all four conformers are given in Table 3.

populations of γ^- rotamers are between 15 to 25 percentage points higher in 4′-thionucleosides **1**–**8** than in their 4′-oxo counterparts, which can be explained by the absence of the *gauche* effect of the [O4′–C4′–C5′–O5′] fragments in the former. The larger population of γ^+ and γ^t over γ^- rotamers in α-4′-thionucleosides **9** and **10** can be explained by the absence of steric repulsions between the nucleobase and 4′-CH_2OH group, which are on opposite sides of the sugar moiety in comparison to their β-anomers. The fact that C–S bonds are *ca.* 0.4 Å longer than C–O bonds suggests that γ^+ rotamers of **1**–**8** exhibit reduced steric hindrance between the 4′-CH_2OH group

and the nucleobase in β-configuration in comparison to their 4′-oxo counterparts. Protonation or deprotonation of the nucleobase is an additional factor that changes the electrostatic attractive interactions of charged heterocyclic aglycon and 5′-OH group and thus influences the conformational equilibria across C4′–C5′ bond at acidic and alkaline pH (Table S2). Interestingly, N7 protonation of guanine nucleobase in both β-tdG (**2**) and β-tG (**6**) caused a significant increase in the population of γ^+ rotamers.

The N⇌S equilibria in **1**–**4** are driven partly by the preference of 3′-OH to adopt a pseudoequatorial (N-type) over pseudoaxial orientation (S-type) sugar conformation. We expected to observe a higher preference for N-type sugar conformation in **1**–**4** due to the absence of the [O4′–C4′–C3′–O3′] *gauche* effect, which is responsible for the stabilisation of S-type pseudorotamers in natural 2′-deoxy-4′-oxonucleosides. Pairwise comparisons did indeed show a higher preference for N-type pseudorotamers, by 13 and 5 percentage points respectively, in β-tdA (**1**) and β-tdG (**2**) compared to β-dA and β-dG at 298 K.[15] In contrast pyrimidine nucleosides showed a slightly higher preference, of 1 and 5 percentage points respectively, for S-type sugar conformation in β-tdC (**3**) and β-tdT (**4**) compared to β-dC and β-T. Pairwise comparisons of $\Delta H°$ values showed that N-type conformers of β-tdA (**1**) and β-tdG (**2**) are stabilised by $\Delta\Delta H°$ of 5.0 and 1.8 kJ mol^{-1}, whereas S-type conformers of β-tdC (**3**) and β-tdT (**4**) are stabilised by $\Delta\Delta H°$ of −0.2 and −0.9 kJ mol^{-1} relative to their natural 4′-oxo counterparts.[15] The above comparisons suggest that 3′-OH prefers pseudoequatorial orientation (achieved in N-type sugar conformation) due to the preference of [S4′–C4′–C3′–O3′] fragments for *trans* over *gauche* conformation alone, but the overall $\Delta G°$ of the N⇌S equilibrium in **1**–**4** is the result of the counteracting anomeric effect, which is highly nucleobase dependent, as well as the competing entropy contributions (Table 2).

The dissection of $\Delta G°$ and $\Delta H°$ of the N⇌S equilibria in 4′-thioribonucleosides **5**–**10** becomes increasingly complex because the 2′-OH group is involved in 1,4 interactions with the nucleobase, S4′ and O3′, and can, in addition, form hydrogen bonds with the neighbouring 3′-OH. The preference of the [S4′–C1′–C2′–O2′] fragment for *trans* over *gauche* conformation drives the N⇌S equilibria of **5**–**10** towards S where the 2′-OH group adopts pseudoequatorial orientation (Figs. 1B and 1D). S-type conformers are energetically preferred due to the *gauche* effect of the [N9/1–C1′–C2′–O2′] fragment in 4′-oxoribonucleosides.[15] Nevertheless β-tA (**5**) and β-tG (**6**) exhibit a higher preference for N-type pseudorotamers, by 13 and 11 percentage points at 298 K and neutral pH, compared to β-A and β-G, respectively. Comparison of $\Delta H°$ values reveals the stabilisation of N-type pseudorotamers in β-tA (**5**) and β-tG (**6**) by 7.5 and 4.7 kJ mol^{-1} compared to β-A and β-G, respectively. In contrast, both β-tC (**7**) and β-tU (**8**) exhibit increased population of S-type sugar conformation by *ca*. 10 percentage points at 298 K and equivalent (within the error limits) $\Delta H°$ values in comparison to β-C and β-U, respectively.

The driving of the N⇌S equilibria in **5**–**8** by the 2′-OH group has been further evaluated by pairwise comparisons of the populations of the S-type pseudorotamers at 278 K and neutral pH between β-tdA (**1**) and β-tA (**5**), β-tdG (**2**) and β-tG (**6**) and β-tdC (**3**) and β-tC (**7**) pairs, which show that there is an additional preference, by 4, 8 and 18 percentage points, for N-type pseudorotamers in 4′-thioribonucleosides, respectively (Table 1). N-Type pseudorotamers are stabilised by $\Delta\Delta H°$ of 2.1, 2.2 and 3.8 kJ mol^{-1} in **5**–**7** relative to **1**–**3**, respectively (Table 2).

S4′-C1′-N9/1 anomeric effect in 1–10

The nucleobase at the anomeric centre drives the N⇌S equilibria in **1**–**10** with two counteracting contributions: (i) steric effects, which are determined by the shape and size of purine or pyrimidine aglycon, and (ii) $n_{S4'} \rightarrow \sigma^*_{C1'\text{-}N}$ interactions (*i.e.* S4′–C1′–N9/1 anomeric effect) which depend on the π-electron density of the individual heterocyclic moiety. The steric interactions of the heterocyclic nucleobase in the β-4′-thionucleosides **1**–**8** are expected to be minimised in the S-type pseudorotamer, where it occupies a pseudoequatorial orientation (Fig. 1B). On the other hand, the S4′–C1′–N9/1 anomeric effect stabilises the N-type sugar conformation in **1**–**8**, where the nucleobase occupies a pseudoaxial orientation (Fig. 1A). In contrast, the α-anomers **9** and **10** show minimal steric effects of the nucleobase in the N-type conformation, where it occupies a pseudoequatorial orientation (Fig. 1C), whereas the opposing S4′–C1′–N9/1 anomeric effect stabilises the S-type sugar conformation, where the nucleobase occupies a pseudoaxial orientation (Fig. 1D).

The only functional variation amongst **1**–**4** is the change of the heterocyclic aglycon and their conformational differences can therefore be attributed to S–C–N anomeric effect. The comparison of $\Delta H°$ values in **1**–**4** shows that the S4′–C1′–N9/1 anomeric effect increases in the following order: thymine < cytosine < guanine < adenine (Table 2). In contrast, the O4′–C1′–N9/1 anomeric effect in 4′-oxonucleosides is weaker in purine than in pyrimidine nucleosides and increases in the following order: adenine < guanine < thymine < cytosine < uracil.[14] If the S4′–C1′–N9/1 anomeric effects in **1**–**4** were of comparable strength to the O4′–C1′–N9/1 anomeric effects in their 4′-oxo counterparts, we should observe a great bias towards the N-type sugar conformation in **1**–**4** because the [S4′–C4′–C3′–O3′] fragment, as well as anomeric effects, drives their N⇌S equilibria towards N-type conformation. We have, however, observed only a minor stabilisation of N-type pseudorotamers in β-tdA (**1**) and β-tdG (**2**) and similar populations of N-type pseudorotamers in β-tdC (**3**) and β-tdT (**4**) relative to their 4′-oxo analogues, which clearly demonstrates that the S4′–C1′–N9/1 anomeric effect is weaker than the O4′–C1′–N9/1 anomeric effect. In 4′-thioribonucleosides **5**–**8** the number and interplay of forces that drive the N⇌S equilibrium is very complex due to additional stereoelectronic effects from 2′-OH group (*vide supra*).

Pairwise comparison of the populations of S-type pseudorotamers at 278 K between α-tA (**9**) and β-tA (**5**), and between α-tU (**10**) and β-tU (**8**) at neutral pH shows that there is a stronger bias, by 33 and 39 percentage points respectively, for N-type conformers in α-4′-thionucleosides **9** and **10** relative to their β-counterparts **5** and **8** (Table 1). The stronger bias towards N-type conformers by $\Delta\Delta H°$ values of 3.2 and 3.3 kJ mol^{-1} for α-tA (**9**) and α-tU (**10**) compared to β-tA (**5**) and β-tU (**8**), respectively suggests that the large steric repulsions between the nucleobase and hydroxy groups on the α-side of α-tA (**9**) and α-tU (**10**) predominate over opposing, but relatively weaker, S4′–C1′–N9/1 anomeric effects and as a result the nucleobase adopts preferentially pseudoequatorial orientation (Table 2).

Effect of protonation and deprotonation on the energetics of the N⇌S equilibria in 1–10

^{1}H NMR chemical shifts of the aromatic and sugar protons of **1**–**10** have been collected at 14–20 pH values in the range from 0.3 to 12.3 (Fig. 2). Comparison of pK_a values of **1**–**10** with their 4′-oxo counterparts showed that substitution of O4′ with S4′ did not change the acid–base character of the constituent heterocyclic moieties. This suggests that the H-bond properties of 4′-thionucleosides **1**–**10** are not affected and thus 4′-thiooligonucleotides form stable duplex structures with complementary RNA or DNA strands.[7–9]

Analysis of the N⇌S pseudorotational equilibria in **1**–**10** as a function of pH also gave sigmoidal plots with pK_a values at the inflection points (Fig. 3). Small population changes were observed upon protonation and deprotonation, except

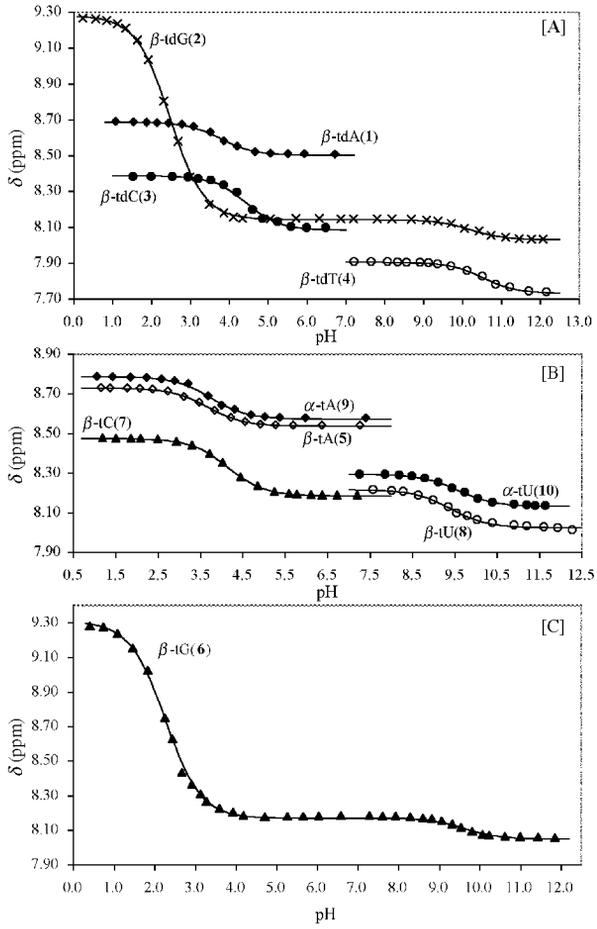

Fig. 2 ^{1}H NMR chemical shifts of the aromatic protons in **1**–**10** as a function of pH (from 0.3 to 12.3 in *ca*. 0.5 unit intervals). Panel [A]: pH-dependent ^{1}H NMR chemical shifts at 298 K for H8 (◆) of *β*-tdA (**1**), H8 (×) of *β*-tdG (**2**), H6 (●) of *β*-tdC (**3**) and H6 (○) of *β*-tdT (**4**). The sigmoidal curves are the best least squares fit for the 15 pH-dependent chemical shifts of *β*-tdA (**1**), 32 of *β*-tdG (**2**), 14 of *β*-tdC (**3**) and 15 of *β*-tdT (**4**) giving the pK_a values of the nucleobases at the inflection points (pK_a = 3.8, δ_P = 8.687 ppm, δ_N = 8.504 ppm, r.m.s. = 0.004 ppm for *β*-tdA (**1**); pK_a = 2.5 and 10.2, δ_P = 9.281 ppm, δ_N = 8.142 ppm, δ_D = 8.031 ppm, r.m.s. = 0.011 ppm for *β*-tdG (**2**); pK_a = 4.4, δ_P = 8.389 ppm, δ_N = 8.084 ppm, r.m.s. = 0.009 ppm for *β*-tdC (**3**) and pK_a = 10.5, δ_N = 7.905 ppm, δ_D = 7.732 ppm, r.m.s. = 0.003 ppm for *β*-tdT (**4**)). Panel [B]: pH-dependent ^{1}H NMR chemical shifts at 298 K for H8 (◇) of *β*-tA (**5**), H6 (▲) of *β*-tC (**7**), H6 (○) of *β*-tU (**8**), H8 (◆) of *α*-tA (**9**) and H6 (●) of *α*-tU (**10**). The sigmoidal curves are the best least squares fit for the 16 pH-dependent chemical shifts of *β*-tA (**5**), 18 of *β*-tC (**7**), 15 of *β*-tU (**8**), 15 of *α*-tA (**9**) and 14 of *α*-tU (**10**) giving the pK_a values of the nucleobases at the inflection points (pK_a = 3.7, δ_P = 8.730 ppm, δ_N = 8.538 ppm, r.m.s. = 0.002 ppm for *β*-tA (**5**); pK_a = 4.2, δ_P = 8.475 ppm, δ_N = 8.184 ppm, r.m.s. = 0.001 ppm for *β*-tC (**7**); pK_a = 9.4, δ_N = 8.216 ppm, δ_D = 8.024 ppm, r.m.s. = 0.005 ppm for *β*-tU (**8**); pK_a = 3.7, δ_P = 8.787 ppm, δ_N = 8.573 ppm, r.m.s. = 0.004 ppm for *α*-tA (**9**) and pK_a = 9.6, δ_N = 8.296 ppm, δ_D = 8.132 ppm, r.m.s. = 0.002 ppm for *α*-tU (**10**)). Panel [C]: pH-dependent ^{1}H NMR chemical shifts at 298 K for H8 (▲) of *β*-tG (**6**). The sigmoidal curve is the best least squares fit using 35 pH-dependent chemical shifts of *β*-tG (**6**) with pK_a values at the inflection points (pK_a = 2.3 and 9.6, δ_P = 9.309 ppm, δ_N = 8.171 ppm, δ_D = 8.049 ppm, r.m.s. = 0.005 ppm).

for β-tdG (**2**) and β-tG (**6**), where the population of S-type conformers at 298 K decreases by 17 and 19 percentage points upon N7 protonation, respectively, and increases by 2 percentage points upon N1 deprotonation (Fig. 3). The change of pH has a great effect on the population of S-type pseudorotamers in α-nucleosides, showing an increase of 17 percentage points upon protonation of α-tA (**9**) and a decrease of 17 percentage points upon deprotonation of α-tU (**10**) at 298 K (Fig. 3). Protonation of β-tdG (**2**) results in stabilisation of the N-type sugar conformations by $\Delta\Delta H°$ of 1.8 kJ mol^{-1}, which can be attributed to the strengthening of the S–C–N anomeric effect

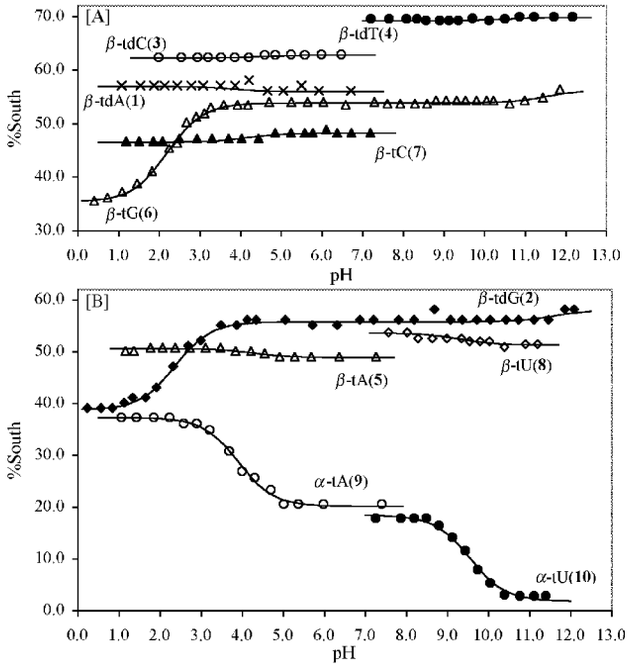

Fig. 3 Population of South-type conformers in **1**–**10** as a function of pH (in *ca*. 0.5 units) at 298 K. Panel [A]: %S and the best fit sigmoidal curves, which gave pK_a values identical to those in Fig. 2 for *β*-tdA (**1**) (×, $\%S_P$ = 57.0, $\%S_N$ = 56.0, r.m.s. = 0.5%), *β*-tdC (**3**) (○, $\%S_P$ = 62.3, $\%S_N$ = 62.8, r.m.s. = 0.1%), *β*-tdT (**4**) (●, $\%S_N$ = 69.2, $\%S_D$ = 69.9, r.m.s. = 0.2%), *β*-tG (**6**) (△, $\%S_P$ = 35.4, $\%S_N$ = 53.9, $\%S_D$ = 56.3, r.m.s. = 0.4%) and *β*-tC (**7**) (▲, $\%S_P$ = 46.6, $\%S_N$ = 48.3, r.m.s. = 0.3%). Panel [B]: %S and the best fit sigmoidal curves, which gave pK_a values identical to those in Fig. 2 for *β*-tdG (**2**) (◆, $\%S_P$ = 38.8, $\%S_N$ = 55.8, $\%S_D$ = 58.0, r.m.s. = 0.6%), *β*-tA (**5**) (△, $\%S_P$ = 50.6, $\%S_N$ = 48.9, r.m.s. = 0.3%), *β*-tU (**8**) (◇, $\%S_N$ = 53.3, $\%S_D$ = 51.3, r.m.s. = 0.4%), *α*-tA (**9**) (○, $\%S_P$ = 37.3, $\%S_N$ = 20.1, r.m.s. = 0.5%) and *α*-tU (**10**) (●, $\%S_N$ = 1.8, $\%S_D$ = 18.4, r.m.s. = 0.5%).

(Table 2). It is noteworthy that $\Delta\Delta H°$ of β-dG upon protonation[29] was 4.9 kJ mol^{-1}, which suggests that the change in the electronic character, which drives sugar conformation, is much reduced in 4′-thionucleosides in comparison to their 4′-oxo counterparts. Protonation of **5**–**8** leads to more positive $\Delta H°$ values, which denote stabilisation of the N-type sugar conformation, except for β-tA (**5**), where the changes are within the error limits. Deprotonation of β-tG (**6**) and β-tU (**8**) results in the stabilisation of the S-type conformers by $\Delta\Delta H°$ of 1.2 and 0.9 kJ mol^{-1}, respectively (Table 2). The S-type pseudorotamers were stabilised by $\Delta\Delta H°$ of −3.6 kJ mol^{-1} upon protonation of α-tA (**9**), which clearly agrees with the strengthening of the anomeric effect.

Conformational equilibrium across the glycosidic bond in 1–10

1D difference NOE experiments were performed to assess the preferred conformation around the glycosidic (C1′–N9/1) bonds in **2**–**10** (Table S5). In **2**–**8** the NOE enhancements at H2′ and H3′ were larger than at H1′ upon saturation of H8/6, which indicates a predominant *anti* orientation of the nucleobase. The pyrimidine bases exhibit larger populations of *anti* conformers in comparison to guanine base. The large NOE enhancement at H4′ upon irradiation of H6 in α-tU (**10**) suggests a high preference for *anti* orientation of the nucleobase. It is noteworthy that the protonation and deprotonation of the nucleobase in **2**–**10** results in no consistent changes in the *syn*⇌*anti* conformational equilibria as a result of conformational cooperativity with N⇌S equilibria or reorientation caused by the change of protonation state.

Ab initio evaluation of the N⇌S pseudorotational equilibria in 1–10

The puckering and energetics of 4′-thiopentofuranose moieties

Table 3 Relative energies and pseudorotational parameters for four distinct conformational states as obtained by *ab initio* MO calculations[a]

Compound	Conformational region	3-21G HF P	3-21G HF Ψ_m	3-21G HF E_{rel}	6-31G** HF P	6-31G** HF Ψ_m	6-31G** HF E_{rel}	6-31G** MP2 E_{rel}	6-31G** PCM E_{rel}	6-31G** NBO^{nostar} E_{rel}
β-tdG (**2**)	North	−4.1	49.2	6.5	2.1	45.9	1.3	0.0	4.4	21.9
	East	90.0	42.8	28.5	90.0	43.5	15.3	20.8	18.0	
	South	173.9	50.2	0.0	172.6	46.4	0.0	1.9	0.0	0.0
	West	280.1	42.7	26.5	280.0	43.4	28.9	16.0	34.8	
β-tdT (**4**)	North	−1.9	48.4	10.4	4.3	45.0	4.2	1.7	9.4	32.3
	East	90.0	42.8	27.4	90.0	43.5	14.0	17.5	13.4	
	South	173.9	50.2	0.0	172.6	46.4	0.0	0.0	0.0	0.0
	West	280.4	41.6	30.5	280.0	43.4	33.1	18.5	34.5	
β-tdU	North	−1.7	48.4	9.8	3.4	45.3	3.6	1.1	3.7	34.8
	East	89.9	42.8	27.7	90.0	43.5	14.4	17.7	14.6	
	South	173.9	50.3	0.0	172.7	46.5	0.0	0.0	0.0	0.0
	West	280.1	42.7	29.7	279.9	43.4	32.1	18.5	33.7	
β-tG (**6**)	North	0.5	48.3	0.0	5.5	45.9	0.0	0.0	0.0	0.0
	East	90.0	43.2	33.0	90.0	43.9	22.1	28.5	21.4	
	South	167.8	43.4	3.7	167.7	46.7	0.4	4.1	0.9	4.9
	West	270.0	43.7	24.7	270.0	44.3	36.7	23.5	39.6	
β-tU (**8**)	North	1.2	48.5	6.6	4.6	46.0	8.1	3.4	3.5	10.1
	East	90.0	43.2	32.7	90.0	43.9	24.0	26.1	21.5	
	South	166.0	50.9	0.0	166.5	47.6	0.0	0.0	0.0	0.0
	West	270.0	43.7	34.2	270.0	44.4	47.3	30.0	44.5	
α-tU (**10**)	North	3.5	49.8	0.0	4.2	48.0	0.0	0.0	0.0	0.0
	East	70.6	44.5	41.3	70.7	45.1	36.3	27.4	34.9	
	South	185.6	40.4	10.7	180.9	39.3	11.8	4.6	9.9	38.3
	West	250.3	44.0	30.0	250.4	44.4	32.6	26.5	36.2	

[a] Both N and S energy minima were obtained through completely free energy minimisations. In the case of the E and W pseudorotamers the endocyclic torsion angles v_2 and v_3 were kept fixed, while all other degrees of freedom were freely optimised. Relative energy (E_{rel}) is given in kJ mol^{-1}. P and Ψ_m are in degrees. PCM denotes polarisable continuum model calculations with water as solvent. NBO^{nostar} is the energy of Lewis structure, where all hyperconjugative interactions are deleted. The lowest energy conformer is arbitrarily taken as 0.0 kJ mol^{-1}. Energies for the lowest energy conformers in au are: −1273.730822 (3-21G), −1280.645851 (6-31G**), −1283.452770 (MP2), −1280.703306 (PCM) and −1278.660721 (NBO^{nostar}) for β-tdG (**2**), −1186.351730 (3-21G), −1192.753392 (6-31G**), −1195.266574 (MP2), −1192.794128 (PCM) and −1191.139075 (NBO^{nostar}) for β-tdT (**4**), −1147.527195 (3-21G), −1153.711219 (6-31G**), −1156.076787 (MP2), −1153.751956 (PCM) and −1152.1715462 (NBO^{nostar}) for β-tdU, −1348.169135 (3-21G), −1355.502722 (6-31G**), −1358.486695 (MP2), −1355.567142 (PCM) and −1353.428671 (NBO^{nostar}) for β-tG (**6**), −1221.965560 (3-21G), −1228.569079 (6-31G**), −1231.110212 (MP2), −1228.617037 (PCM) and −1226.937167 (NBO^{nostar}) for β-tU (**8**) and −1221.970165 (3-21G), −1228.571792 (6-31G**), −1231.112267 (MP2), −1228.620276 (PCM) and −1226.943181 (NBO^{nostar}) for α-tU (**10**).

have been examined by *ab initio* molecular orbital calculations on β-tdG (**2**), β-tdT (**4**), β-tdU, β-tG (**6**), β-tU (**8**) and α-tU (**10**) at HF and MP2 levels of theory. First, we performed a series of pseudorotational energy profile calculations at HF/3-21G level in such a way to scan the conformational space from W *via* N and E to S regions at maximum puckering amplitude of 49°. The plots of relative energy as a function of P in Fig. 4 clearly show two energy wells in the N and S regions of conformational space. The two lowest energy conformers at the HF/3-21G level were used as input for completely free optimisations at the HF/6-31G** level (Table 3). Further calculations were performed by the inclusion of electron correlation at the MP2/6-31G** level and with PCM to mimic water solvation. Natural bond orbital (NBO) analysis with the deletion of all hyperconjugative interactions showed great energetic destabilisation of N-type pseudorotamers for β-4′-thionucleosides, which indicates that the nonbonding interactions are more efficient in N-type sugar conformation, which is stabilised by anomeric effect. A great energetic stabilisation of N-type pseudorotamer has been observed for α-tU (**10**) upon deletion of all nonbonding orbitals together with the anomeric effect, which stabilises S-type pseudorotamers (Table 3). As the anomeric effect can be attributed to the stabilising 2-electron $n_{S4'} \rightarrow \sigma^*_{C1'-N}$ hyperconjugation we have deleted this interaction in further NBO analysis and found greater destabilisation by 1.1 and 3.0 kJ mol^{-1} in β-tdG (**2**) and β-tG (**6**) compared to β-tdU and β-tU(**8**), respectively, which has suggested stronger anomeric effect in purine than in pyrimidine 4′-thionucleosides.

The lowest energy conformers of 4′-thionucleosides in the N and S regions of conformational space, which were completely freely optimised, exhibited puckering around C3′-*endo* and between C2′-*endo* and C2′-*endo*, C3′-*exo* canonical forms, respectively (Table 3). These results are comparable to those obtained from NMR analysis. The C–S bonds are *ca*. 0.4 Å longer than the C–O bonds, which causes the extrusion of endocyclic S4′ atom from the plane of pentofuranosyl ring and results in the increase of the puckering amplitude (Ψ_m) up to 51° in **1**–**10** compared to natural nucleosides.

The pseudorotational energy profiles at the HF/3-21G level suggested an energy barrier between 27.4 and 41.3 kJ mol^{-1} in the E-region of conformational space (Fig. 4). When the E pseudorotamers were reoptimised at the HF/6-31G** level the energy barriers were lowered to 14.0–36.3 kJ mol^{-1} (Table 3). Interestingly, the barrier in the W region is not much higher or is even lower for β-tdG (**2**), β-tG (**6**) and α-tU (**10**) than the barrier in the E region of conformational space in contrast to 4′-oxoribonucleotides, where the barriers in the E region of conformational space are much lower than in the W region. This can be attributed to the smaller steric hindrance in the W-type conformers of 4′-thioribonucleosides compared to their 4′-oxo counterparts due to longer S4′–C1′ and C4′–S4′

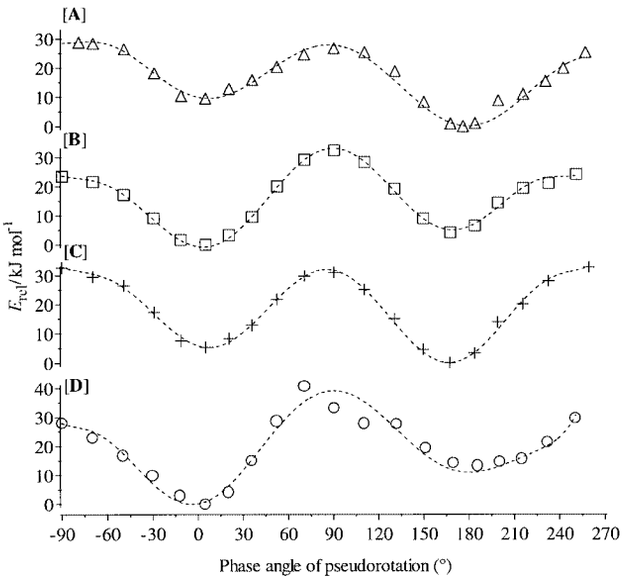

Fig. 4 The plots of *ab initio* relative energy as a function of the phase angle of pseudorotation (*P*) at HF/3-21G level for *β*-tdU in panel [A], for *β*-tG (**6**) in panel [B], for *β*-tU (**8**) in panel [C] and for *α*-tU (**10**) in panel [D]. The energy profiles have been obtained through 22 optimisations for *β*-tdU and 20 optimisations for *β*-tG (**6**), *β*-tU (**8**) and *α*-tU (**10**) at the HF/3-21G level by keeping only ν_2 and ν_3 frozen to appropriate values to *P* in the range from 0 to 340° in *ca*. 20° steps at $\Psi_m = 49°$, while all other degrees of freedom were freely optimised. The lowest energy conformer in all four panels was arbitrarily taken as 0.0 kJ mol^{-1}.

bonds compared to O4′–C1′ and C4′–O4′ bonds. The *ab initio* calculated energy barriers suggest a rapid exchange between the interconverting conformers on the NMR time scale which results in the time-averaged chemical shifts and coupling constants in 4′-thionucleosides **1**–**10**.

Experimental

NMR spectroscopy

^{1}H NMR spectra were recorded at 299.942 MHz on Varian Unity Plus and at 600.113 MHz on Varian Unity Inova NMR spectrometer at the National NMR Center of Slovenia. Spectra were acquired in D_2O (99.9% deuterium) at five temperatures from 278 to 358 K (±0.5 K) in 20 K steps. Sample concentrations were 10 mM for β-tdC (**3**), β-tdT (**4**), β-tC (**7**), β-tU (**8**) and α-tU (**10**), 5 mM for β-tdG (**2**), β-tG (**6**) and α-tA (**9**), and 2.5 mM for β-tdA (**1**) and β-tA (**5**) due to poor solubility. In order to obtain accurate *J*-coupling data and chemical shifts ^{1}H NMR spectra were simulated with a standard computer simulation algorithm, which is integrated into Varian software (VNMR rev. 6.1A).[30] The error in $^3J_{HH}$ is smaller than 0.1 Hz as estimated from the comparison of the experimental and simulated spectra.

Conformational analysis of $^3J_{HH}$

The conformational analysis of the thiofuranose moiety in **1**–**10** has been performed with the use of computer program PSEUROT,[31] which finds the best fit between experimental and calculated $^3J_{HH}$. The input consists of the parameters P_1–P_6 for the generalised Karplus–Altona equation, the λ electronegativities of the four substituents, *A*, *B*, a_j and ε_j parameters, temperature-dependent experimental $^3J_{HH}$ and the initial guesses of the geometries of the starting conformers and their respective populations. The following λ electronegativity values were used: 0.0 for H, 1.26 for OH, 0.62 for C1′, C2′, C3′ and C4′, 0.68 for C5′, 0.70 for S and 0.58 for the nucleobase. Parameters *A* and *B*, and parameters a_j and ε_j for **1**–**10** are given in Tables S3 and S4.

Ab initio MO calculations

All calculations were performed with GAUSSIAN 94[32] and 98[33] program. Standard basis sets were used as implemented in Gaussian programs. For all the pseudorotamers all internal degrees of freedom were first freely optimised at Hartree–Fock (HF) level of theory using the standard 3-21G basis set. For the calculation of the energy profile shown in Fig. 4, endocyclic torsion angles ν_2 and ν_3 were kept fixed to scan the conformational space.[24] HF/3-21G optimised geometries of the N-, E-, S-, and W-type conformers were used as input for geometry optimisations at HF/6-31G** level. The energy calculations were performed with the inclusion of the electron correlation using the second-order Møller–Plesset (MP2) theory. Calculations with polarisable continuum model[34] were performed to evaluate the effect of aqueous medium. Number of the tessarea per sphere in all PCM calculations was 60, except for *β*-tdG (**7**) where it was 80 to achieve convergence. Natural bond orbital (NBO)[35] analysis has been used to evaluate delocalisation effects. Stationary points were verified through vibrational frequency calculations.

Acknowledgements

We thank the Ministry of Science and Technology of the Republic of Slovenia (Grant No. Z1-8609-0104) and Krka, Pharmaceutical and Chemical Works, Novo mesto, Slovenia for their financial support and for their financial contribution for the purchase of 300 and 600 MHz Varian NMR spectrometers. We are grateful to Dr J. A. Secrist for a generous gift of the 4′-thio-2′-deoxynucleosides.

References

1 N. A. Van Draanen, G. A. Freeman, S. A. Short, R. Harvey, R. Jansen, G. Szczech and G. W. Koszalka, *J. Med. Chem.*, 1996, **39**, 538.
2 S. G. Rahim, N. Trivedi, M. V. Bogunivich-Batchelor, G. W. Hardy, G. Mills, J. W. T. Sellway, W. Snowden, E. Littler, P. L. Coe, I. Basnak, R. F. Whale and R. T. Walker, *J. Med. Chem.*, 1996, **39**, 789.
3 M. A. Clement and S. H. Berger, *Med. Chem. Res.*, 1992, **2**, 154.
4 M. I. Elzagheid, M. Oivanen, R. T. Walker and J. A. Secrist, *Nucleosides Nucleotides*, 1999, **18**, 181.
5 C. Leydier, L. Bellon, J.-L. Barascut and J.-L. Imbach, *Nucleosides Nucleotides*, 1995, **14**, 1027.
6 C. Leydier, L. Bellon, J.-L. Barascut, F. Morvan, B. Rayner and J. L. Imbach, *Antisense Research Development*, 1995, **5**, 167.
7 D. Dukhan, F. De Valette, R. Marquet, B. Ehresmann, C. Ehresmann, F. Morvan, J.-L. Barascut and J. L. Imbach, *Nucleosides Nucleotides*, 1999, **18**, 1423.
8 S. Kumar, J. R. Horton, G. D. Jones, R. T. Walker, R. J. Roberts and X. Cheng, *Nucleic Acids Res.*, 1997, **25**, 2773.
9 G. D. Jones, E. A. Lesnik, S. R. Owens, L. M. Risen and R. T. Walker, *Nucleic Acids Res.*, 1996, **24**, 4117.
10 F. Debart, G. Tosquellas, B. Rayner and J.-L. Imbach, *Nucleosides Nucleotides*, 1995, **14**, 1015.
11 W. Saenger, *Principles of Nucleic Acid Structure*, Springer Verlag, New York, 1984.
12 C. Altona and M. Sundaralingam, *J. Am. Chem. Soc.*, 1972, **94**, 8205.
13 C. Altona and M. Sundaralingam, *J. Am. Chem. Soc.*, 1973, **95**, 2333.
14 C. Thibaudeau and J. Chattopadhyaya, *Stereoelectronic Effects in Nucleosides and Nucleotides and their Structural Implications*, Uppsala University Press, Uppsala, Sweden, 1999.
15 J. Plavec, W. Tong and J. Chattopadhyaya, *J. Am. Chem. Soc.*, 1993, **115**, 9734.
16 M. Polak, B. Mohar, J. Kobe and J. Plavec, *J. Am. Chem. Soc.*, 1998, **120**, 2508.
17 E. Juaristi and G. Cuevas, *Tetrahedron*, 1992, **48**, 5019.
18 I. Tvaroska and T. Bleha, in *Anomeric and exo-anomeric effects in carbohydrate chemistry*, ed. R. S. Tipson and D. Horton, San Diego, 1989.
19 A. J. Kirby and N. H. Williams, in *Anomeric and Gauche Effects*, ed. G. R. J. Thatcher, Washington, DC, 1993.

20 L. H. Koole, J. Plavec, H. Liu, B. R. Vincent, M. R. Dyson, P. L. Coe, R. T. Walker, G. W. Hardy, G. S. Rahim and J. Chattopadhyaya, *J. Am. Chem. Soc.*, 1992, **114**, 9936.
21 C. A. G. Haasnoot, F. A. A. M. de Leeuw and C. Altona, *Tetrahedron*, 1980, **36**, 2783.
22 C. Altona, R. Francke, R. de Haan, J. H. Ippel, G. J. Daalmans, A. J. A. Westra Hoekzema and J. van Wijk, *Magn. Reson. Chem.*, 1994, **32**, 670.
23 F. A. A. M. de Leeuw and C. Altona, *J. Comput. Chem.*, 1983, **4**, 428.
24 The endocyclic torsion angles in **1**–**10** are defined as follows: ν_0 = [C4′–S4′–C1′–C2′], ν_1 = [S4′–C1′–C2′–C3′], ν_2 = [C1′–C2′–C3′–C4′], ν_3 = [C2′–C3′–C4′–S4′] and ν_4 = [C3′–C4′–S4′–C1′].
25 E. Diez, A. L. Esteban, F. J. Bermejo, C. Altona and F. A. A. M. de Leeuw, *J. Mol. Struct.*, 1984, **125**, 49.
26 Structural parameters for two completely freely MP2/6-311++G** optimised conformers of 2-methylthioethanol are as follows: r(C–S) = 1.812, r(C–C) = 1.519, r(C–O) = 1.426 Å for *trans* (179.9°) and r(C–S) = 1.812, r(C–C) = 1.517, r(C–O) = 1.424 Å for *gauche* (−63.5°) rotamer.
27 J. Mullay, *J. Am. Chem. Soc.*, 1985, **107**, 7271.
28 N. Inamoto and S. Masuda, *Chem. Lett.*, 1982, 1003.
29 C. Thibaudeau, J. Plavec and J. Chattopadhyaya, *J. Org. Chem.*, 1996, **61**, 266.
30 Varian *VNMR™ data acquisition and processing software*, revision 6.1A, Varian, Palo Alto, 1999.
31 C. Haasnoot, F. A. A. M. de Leeuw, D. Huckriede, J. van Wijk and C. Altona *PSEUROT—A program for the conformational analysis of five membered rings*, version 6.0, Leiden University, Leiden, Netherlands, 1993.
32 M. J. Frisch, G. W. Trucks, H. B. Schlegel, P. M. W. Gill, B. G. Johnson, M. A. Robb, J. R. Cheeseman, T. Keith, G. A. Petersson, J. A. Montgomery, K. Raghavachari, M. A. Al-Laham, V. G. Zakrzewski, J. V. Ortiz, J. B. Foresman, J. Cioslowski, P. B. Stefanov, A. Nanayakkara, M. Challacombe, C. Y. Peng, P. Y. Ayala, W. Chen, M. W. Wong, J. L. Andres, E. S. Replogle, R. Gomperts, R. L. Martin, D. J. Fox, J. S. Binkley, D. J. Defrees, J. Baker, J. P. Stewart, M. Head-Gordon, C. Gonzalez and J. A. Pople, *Gaussian 94*, Revision D.1, Gaussian Inc., Pittsburgh, PA, 1995.
33 M. J. Frisch, G. W. Trucks, H. B. Schlegel, G. E. Scuseria, M. A. Robb, J. R. Cheeseman, V. G. Zakrzewski, J. A. Montgomery, R. E. Stratmann, J. C. Burant, S. Dapprich, J. M. Millam, A. D. Daniels, K. N. Kudin, M. C. Strain, O. Farkas, J. Tomasi, V. Barone, M. Cossi, R. Cammi, B. Mennucci, C. Pomelli, C. Adamo, S. Clifford, J. Ochterski, G. A. Petersson, P. Y. Ayala, K. M. Q. Cui, D. K. Malick, A. D. Rabuck, K. Raghavachari, J. B. Foresman, J. Cioslowski, J. V. Ortiz, B. B. Stefanov, G. Liu, A. Liashenko, P. Piskorz, I. Komaromi, R. Gomperts, R. L. Martin, D. J. Fox, T. Keith, M. A. Al-Laham, C. Y. Peng, A. Nanayakkara, C. Gonzalez, M. Challacombe, P. M. W. Gill, B. G. Johnson, W. Chen, M. W. Wong, J. L. Andres, M. Head-Gordon, E. S. Replogle and J. A. Pople, *Gaussian 98*, Revision A.5, Gaussian Inc., Pittsburgh, PA, 1998.
34 V. Barone, M. Cossi and J. Tomasi, *J. Chem. Phys.*, 1997, **107**, 3210.
35 A. E. Reed, L. A. Curtiss and F. Weinhold, *Chem. Rev.*, 1988, **88**, 899.

Paper a908096a